PNAS

Supporting Information for

Southern Ocean drives multi-decadal atmospheric CO_2 rise during Heinrich Stadials

Kathleen A. Wendt*, Christoph Nehrbass-Ahles, Kyle Niezgoda, David Noone, Michael Kalk, Laurie Menviel, Julia Gottschalk, James Rae, Jochen Schmitt, Hubertus Fischer, Thomas F. Stocker, Juan Muglia, David Ferreira, Shaun A. Marcott, Edward Brook, and Christo Buizert

*Corresponding author: Kathleen Wendt
Email: Kathleen.wendt@oregonstate.edu

This PDF file includes:

Supporting text
Figures S1 to S8
Tables S1 to S3
Legends for Datasets S1 to S2
SI References

Other supporting materials for this manuscript include the following:

Datasets S1 to S2

Supporting Information Text

Isotope-enabled modeling

Shifts in the SH westerlies. The Southern Ocean response to an intensification of the SH westerlies occurs on two timescales (Ferreira et al., 2015; Kostov et al., 2017). The immediate response (0 to ~5 years) to an increase in SH westerly wind stress (a positive shift in Southern Annular Mode [SAM] index) is an intensification of northward Ekman drift, resulting in SST cooling and sea ice expansion around Antarctica. The long-term response (>10 years) relies on upwelling of warm waters from below the mixed layer which can result in SST warming (Ferreira et al., 2015; Kostov et al., 2017).

Much published work focuses on the short-term response, which is not applicable to both HS and HE where we expect a persistent shift in the SH westerlies on longer timescales. It is challenging to derive the long-term SST and SIC response from observational data or unforced climate model simulations, because responses are dominated by internal variability in SAM on monthly to interannual timescales (Thompson & Wallace, 2000). A response function approach can be used to estimate the long-term SH westerly response from unforced internal variability. Applying this approach to SST (Kostov et al., 2017) or SIC (Holland et al., 2017) suggests that climate models exhibit a widespread difference in the timing, sign, and magnitude of the long-term response, due to for example differences in Southern Ocean thermal stratification.

Modeling Southern Ocean sea ice anomalies. The sea ice (SIC) response to an intensification of the SH westerlies (positive SAM) is more complex than the SST response, as the sea ice distribution is impacted by both mechanical (i.e., wind stress) and thermal forcing (Lefebvre et al., 2004), and has a complex, zonally-asymmetrical response to shifting westerlies (Lefebvre et al., 2004; Sen Gupta & England, 2006) which may drive regional sea ice expansion despite an increase in SST. Models and observations typically show a zonally asymmetrical short-term sea ice response, with decreased sea ice in the Weddell Sea, and increased sea ice in the Ross and Amundsen Seas during positive SAM phase (Lefebvre et al., 2004; Sen Gupta & England, 2006). In most climate models, the initial response to a positive SAM shift is an expansion of Antarctic sea ice due to enhanced northward Ekman transport and SST cooling (Holland et al., 2017). On longer timescales, however, SST warming may reduce the SIC. This is what happens in the aforementioned wind forcing experiments by Menviel et al. (2018). The thermal response is likely dependent on the location and mechanism of any SST warming.

Fig. S6 shows the isotopic response to an idealized sea ice forcing where at each latitude the sea ice edge is displaced poleward such that 20% of the total sea ice cover at that latitude is removed. The impact of the SIC anomaly on water isotopes is greatest on the ice sheet margin (Noone & Simmonds, 2004), where it is characterized by warming, enrichment in $\delta^{18}O$, and depletion in d_{ln}. Experiments with increased sea ice extent (not shown) give the opposite pattern as expected. Overall, a reduction in Antarctic sea ice extent deteriorates the fit to observations while an increase in sea ice improves the fit. The opposing $\delta^{18}O$ and d_{ln} changes simulated for SIC anomalies contrast with the ice core observations, where Antarctic $\delta^{18}O$ and d_{ln} both show positive anomalies during Heinrich events. From our simulations, the ice core observations are most easily explained by SST warming and an absence of a strong sea ice response. The latter may be due to the fact that the SST anomalies occur northward of the sea ice edge, or because the mechanical- and thermal impacts of a shift in the SH westerlies oppose one another out to produce little net change in sea ice.

Heinrich Stadial*	Associated depth in WD** (m)	Average temporal resolution at selected depth (yrs/m)	Sampling resolution (m)	Temporal resolution (yrs)	Average absolute age uncertainty (yrs)
H2	2625 – 2650	32	0.2 – 1	10 – 70	270
H3	2815 – 2850	36	0.3 – 2	10 – 70	314
H4	3040 – 3060	44	0.1 – 1	2 – 50	355
H5	3210 – 3230	58	0.2 –1	10 – 70	376

*Timing and duration of HSs outlined in Martin et al. (2023)
**Associated variations in WD CH_4

Table S1: WD sampling intervals and resolution.

Heinrich Stadial	Selected interval (yrs BP)		Identified rise interval (yrs BP)		Rise duration (yrs)	Rise in CO_2 (ppm)
	Start	*End*	*Start*	*End*		
1	16600	15300	16160 ± 176	16084 ± 172	76 ± 23	12 ± 0.7
2	24350	24050	24106 ± 272	24093 ± 271	14 ± 10	7 ± 1.2
3	30600	29950	30335 ± 328	30211 ± 328	124 ± 74	4 ± 0.9
4	39900	39100	39546 ± 379	39491 ± 377	55 ± 10	14 ± 0.8
5	48600	48260	48441 ± 382	48293 ± 382	148 ± 50	8 ± 1.4
Stacked (1-5)					103 ± 50	7 ± 1.4
Stacked (1, 4, 5)					87 ± 50	10 ± 1.4

Table S2: RAMPFIT analysis results, including stacked records of (1) HSs 1-5 and (2) the three largest magnitude HSs (HS 1, 4, 5).

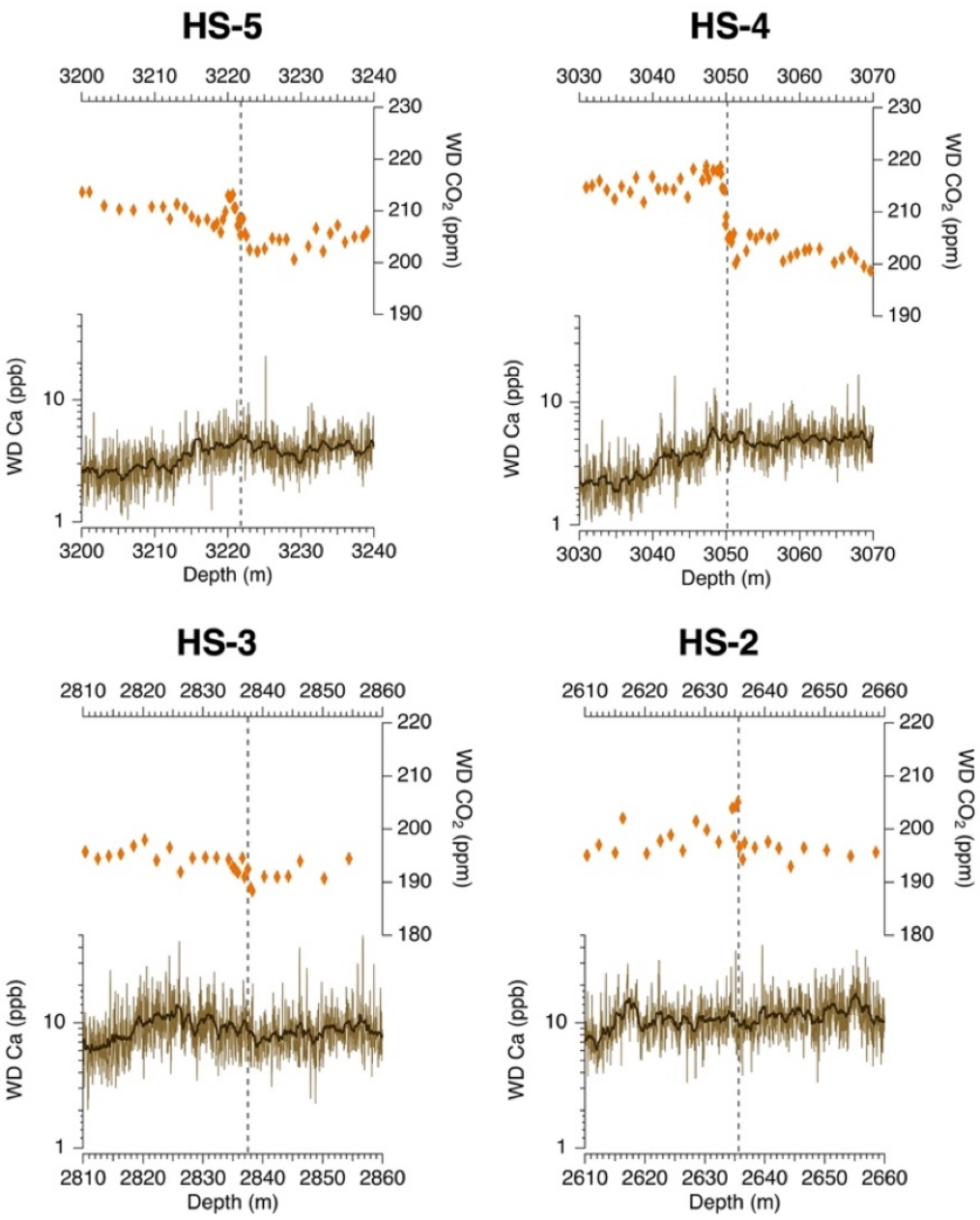

Figure S1: WD CO_2 from (Bauska et al., 2021) (orange) and this study (red) and WD Ca concentrations in the ice phase shown on a logarithmic scale (light brown) (Markle et al., 2018) with overlaying cubic spline (dark brown). Vertical line indicates timing of interpreted CO_2 jumps.

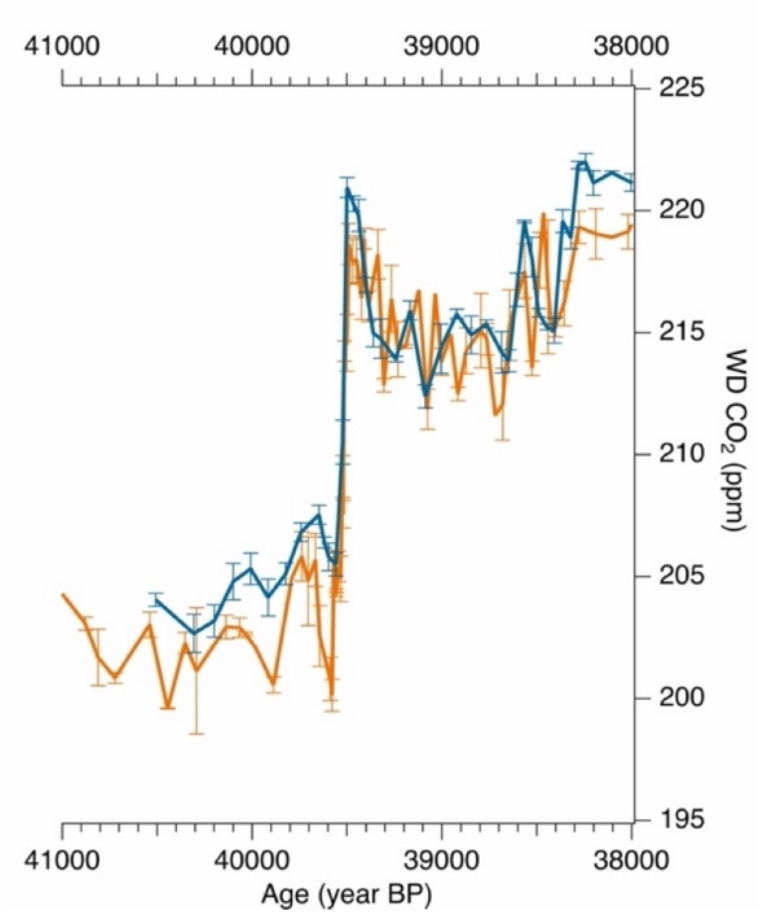

Figure S2: CO_2 measurements from the University of Bern using a Centrifugal Ice Microtome (blue) and from Oregon State University using a steel pin crusher (orange) over same time interval. Uncertainties are 1σ deviations of 2-4 individual measurements per depth. BP = before present, where "present" is the year 1950.

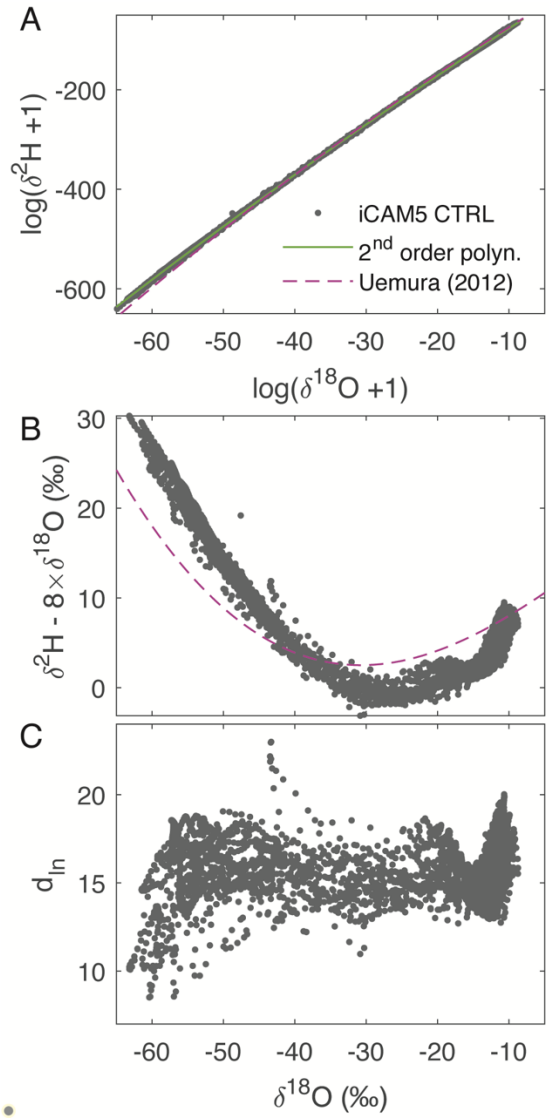

Figure S3: Relationship between Antarctic (a) ln(1+$\boldsymbol{\delta}^{18}$O) and ln(1+$\boldsymbol{\delta}^{2}$H), (b) $\boldsymbol{\delta}^{2}$H -8x$\boldsymbol{\delta}^{18}$O and $\boldsymbol{\delta}^{18}$O, and (c) d_{ln} and $\boldsymbol{\delta}^{18}$O in iCAM5 LGM control run (black circles), using a 2nd order polynomial fit south of 45°S in the iCAM5 LGM control run (green), and using the Uemura et al. (2012) d_{ln} definition (dashed purple).

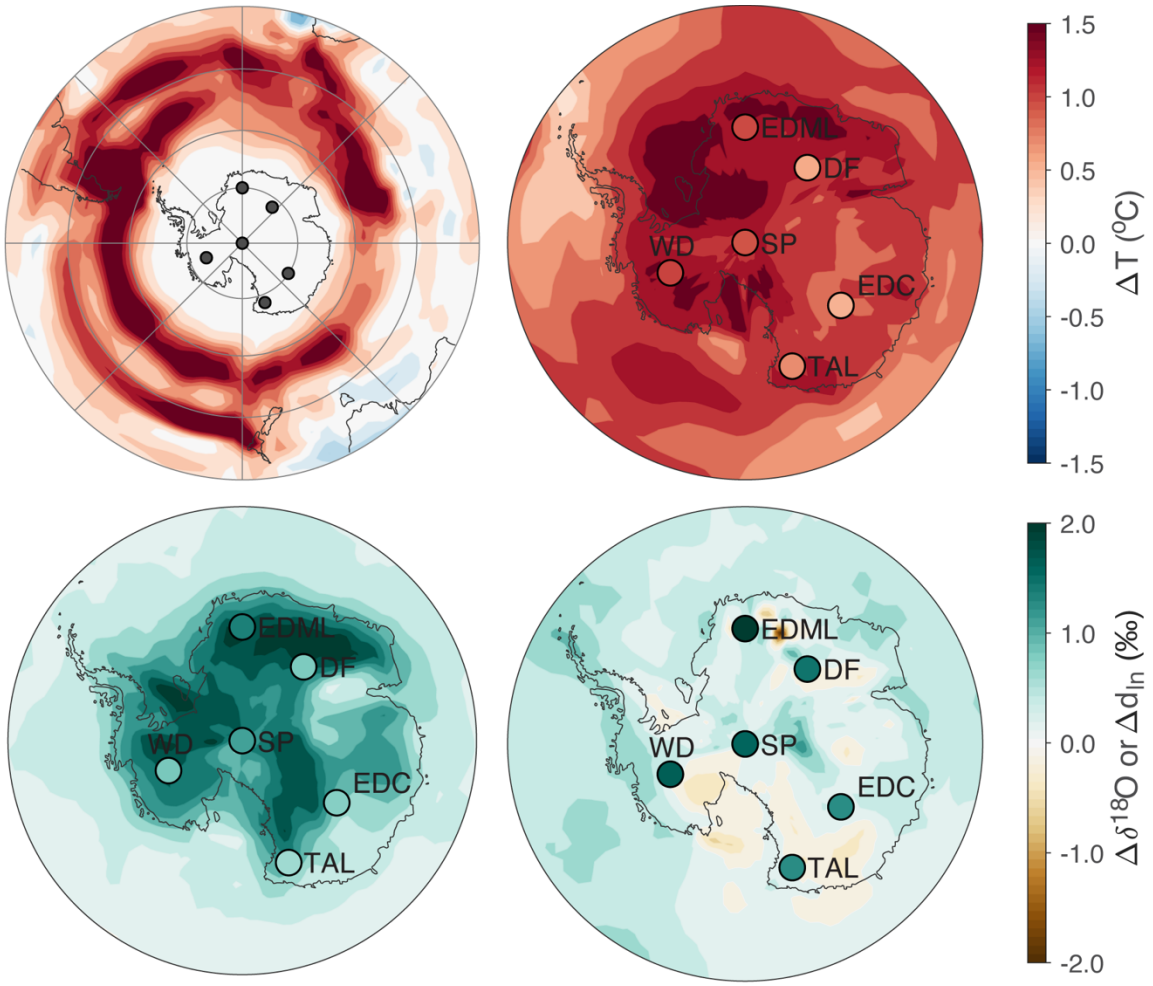

Figure S4: iCAM5 simulated change in temperature (upper right) and change in the $\boldsymbol{\delta}^{18}$O (lower left) and d_{ln} (lower right) of Antarctic precipitation using the SST response from Menviel et al. (2018) (upper left) to a simulated southward shift of the SH westerlies around 16.3 ka BP in the LOVECLIM Earth system model. Relative change in temperature and water isotopes recorded in respective ice cores indicated by dot.

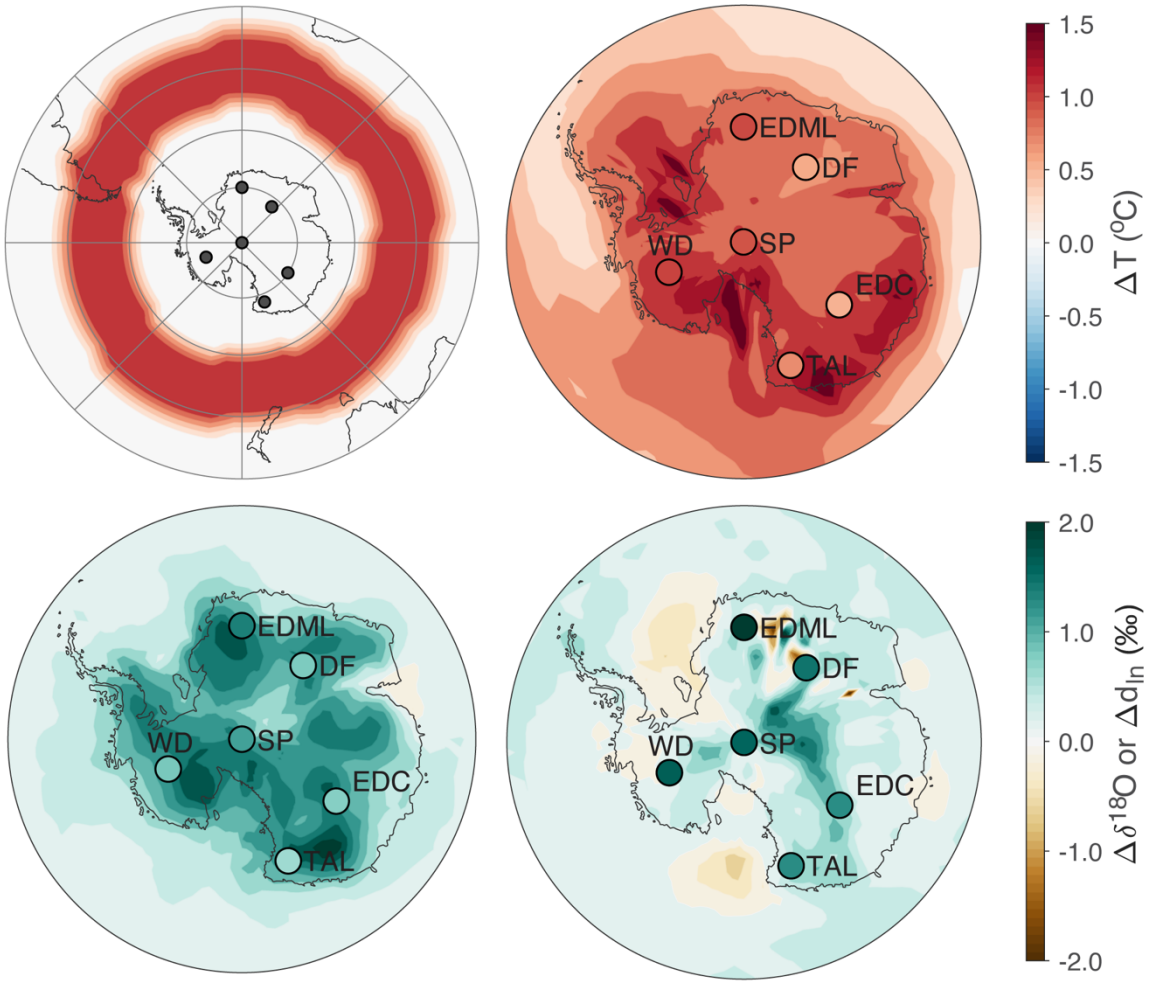

Figure S5: iCAM5 simulated change in temperature (upper right) and change in the $\boldsymbol{\delta}^{18}$O (lower left) and d_{ln} (lower right) of Antarctic precipitation using idealized SST anomaly that consists of a 1°C SST warming in a latitudinal band that is 15 degrees wide (upper left), the southern edge of which is placed just north of the wintertime sea ice edge (to avoid applying any warming underneath the sea ice). Relative change in temperature and water isotopes recorded in respective ice cores indicated by dot.

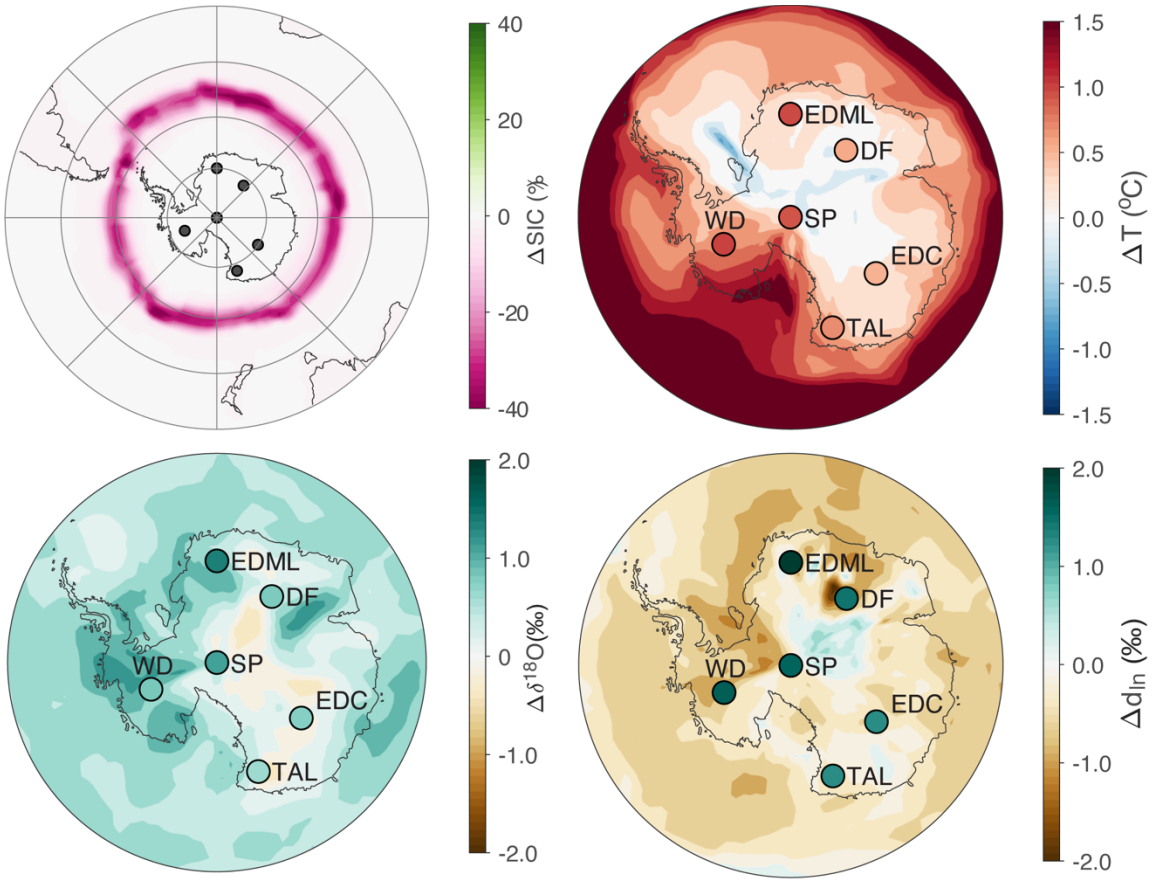

Figure S6: iCAM5 simulated change in temperature (upper right) and change in the $\boldsymbol{\delta}^{18}O$ (lower left) and d_{ln} (lower right) of Antarctic precipitation using an idealized sea ice forcing where at each latitude the sea ice edge is displaced poleward such that 20% of the total sea ice cover at that latitude is removed. Change in percentage of sea ice cover (SIC) upper left. Relative change in temperature and water isotopes recorded in respective ice cores indicated by dot.

	Ferreira x2 SST **Fig. 4**	**Ferreira x1 SST** **Not shown**	**Menviel SST** **Fig. S4**	**Idealized SST** **Fig. S5**	**Idealized SIC** **Fig. S6**
ΔT (°C)	0.37	0.60	0.14	0.22	0.61
$\Delta\boldsymbol{\delta}^{18}O$ (‰)	0.45	0.74	0.29	0.47	0.66
Δd_{ln} (‰)	1.45	1.50	1.23	1.27	2.25

Table S3: Root mean square deviation of applied SST anomaly and SIC forcing model results from observed changes in ice core proxies.

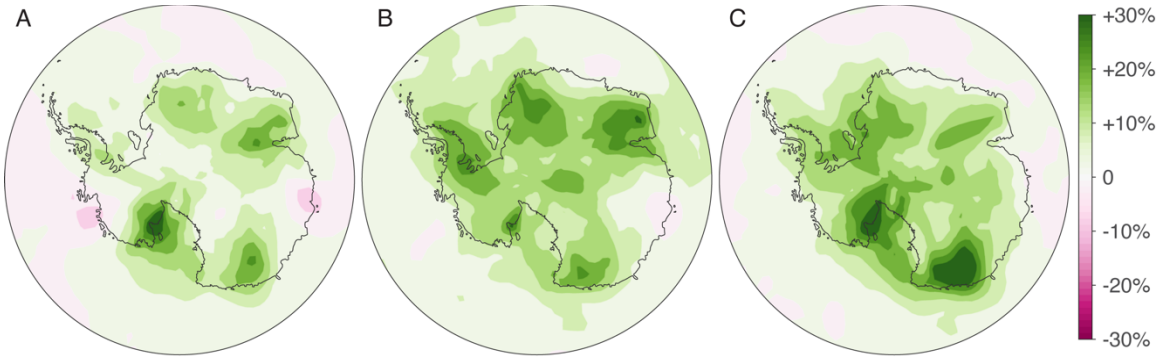

Figure S7: iCAM5 simulated relative change in annual-mean precipitation under the three SST warming scenarios: (A) Ferreira et al. (2015); (B) Menviel et al. (2018); (C) idealized 1ºC SST warming.

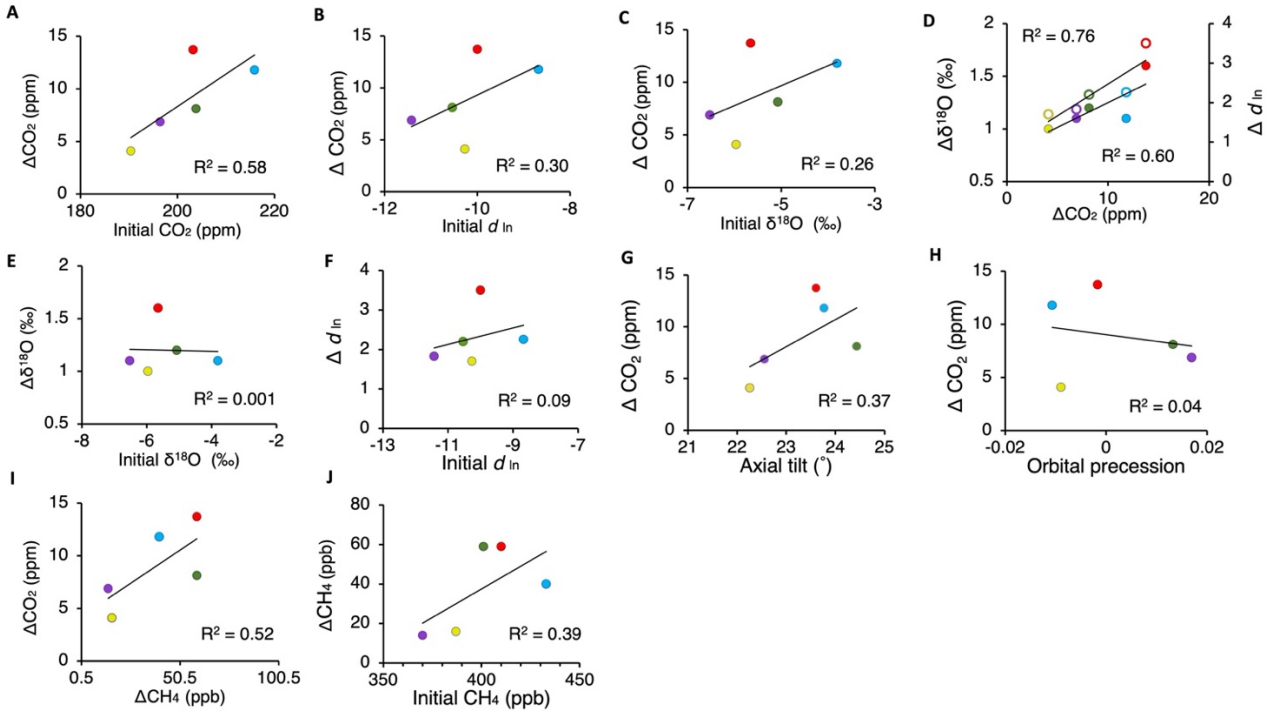

Figure S8: Scatter plots showing the magnitude of change in CO_2 concentrations (ΔCO_2), CH_4 concentrations (ΔCH_4), $\delta^{18}O$ ($\Delta\delta^{18}O$), and d_{ln} (Δd_{ln}) versus the initial value of CO_2, CH_4, $\delta^{18}O$, and d_{ln} prior to mid-stadial event associated with HS-1 (blue), HS-2 (purple), HS-3 (yellow), HS-4 (red), and HS-5 (green). $\Delta\delta^{18}O$ represented by filled circles and Δd_{ln} represented by open circles in plot D. Scatter plots G and H show the magnitude of change in CO_2 concentrations versus Earth's axial tilt and precessional index (Berger & Loutre, 1991) at the time of mid-HS CO_2 jumps.

Dataset S1 (separate file). WAIS Divide Replicate (Core WDC-R1) CO_2 amount fractions measured at the University of Bern

Dataset S2 (separate file). WAIS Divide (WD06A) core CO_2 amount fractions measured at Oregon State University

SI References

Bauska, T. K., Marcott, S. A., & Brook, E. J. (2021). Abrupt changes in the global carbon cycle during the last glacial period. *Nature Geoscience*, *14*(2), 91-96.

Berger, A., & Loutre, M.-F. (1991). Insolation values for the climate of the last 10 million years. *Quaternary Science Reviews*, *10*(4), 297-317.

Ferreira, D., Marshall, J., Bitz, C. M., Solomon, S., & Plumb, A. (2015). Antarctic Ocean and sea ice response to ozone depletion: A two-time-scale problem. *Journal of Climate*, *28*(3), 1206-1226.

Holland, M. M., Landrum, L., Kostov, Y., & Marshall, J. (2017). Sensitivity of Antarctic sea ice to the Southern Annular Mode in coupled climate models. *Climate Dynamics*, *49*, 1813-1831.

Kostov, Y., Marshall, J., Hausmann, U., Armour, K. C., Ferreira, D., & Holland, M. M. (2017). Fast and slow responses of Southern Ocean sea surface temperature to SAM in coupled climate models. *Climate Dynamics*, *48*, 1595-1609.

Lefebvre, W., Goosse, H., Timmermann, R., & Fichefet, T. (2004). Influence of the Southern Annular Mode on the sea ice–ocean system. *Journal of Geophysical Research: Oceans*, *109*(C9).

Markle, B. R., Steig, E. J., Roe, G. H., Winckler, G., & McConnell, J. R. (2018). Concomitant variability in high-latitude aerosols, water isotopes and the hydrologic cycle. *Nature Geoscience*, *11*(11), 853-859.

Martin, K. C., Buizert, C., Edwards, J. S., Kalk, M. L., Riddell-Young, B., Brook, E. J., Beaudette, R., Severinghaus, J. P., & Sowers, T. A. (2023). Bipolar impact and phasing of Heinrich-type climate variability. *Nature*, *617*(7959), 100-104.

Menviel, L., Spence, P., Yu, J., Chamberlain, M., Matear, R., Meissner, K., & England, M. H. (2018). Southern Hemisphere westerlies as a driver of the early deglacial atmospheric CO2 rise. *Nature communications*, *9*(1), 2503.

Noone, D., & Simmonds, I. (2004). Sea ice control of water isotope transport to Antarctica and implications for ice core interpretation. *Journal of Geophysical Research: Atmospheres*, *109*(D7).

Sen Gupta, A., & England, M. H. (2006). Coupled ocean–atmosphere–ice response to variations in the southern annular mode. *Journal of Climate*, *19*(18), 4457-4486.

Thompson, D. W., & Wallace, J. M. (2000). Annular modes in the extratropical circulation. Part I: Month-to-month variability. *Journal of Climate*, *13*(5), 1000-1016.

Uemura, R., Masson-Delmotte, V., Jouzel, J., Landais, A., Motoyama, H., & Stenni, B. (2012). Ranges of moisture-source temperature estimated from Antarctic ice cores stable isotope records over glacial–interglacial cycles. *Climate of the Past*, *8*(3), 1109-1125.